

# Detecting $h_c(^1P_1)$ at the LHC

Cong-Feng Qiao

*Department of Physics, Graduate University, the Chinese Academy of Sciences  
YuQuan Road 19A, 100049, Beijing, China and  
Theoretical Physics Center for Science Facilities (TPCSF), CAS*

De-Long Ren and Peng Sun

*Department of Physics, Graduate University, the Chinese Academy of Sciences  
YuQuan Road 19A, 100049, Beijing, China*

## Abstract

In this work, we calculate the  $h_c(^1P_1)$  production rate at the LHC to leading order of the strong coupling constant, for both color-singlet and -octet mechanisms. Numerical results show that a considerable number of  $h_c$  events with moderate transverse momentum  $p_T$  will be produced in the early run of the LHC, which will supply a good opportunity to further study the nature of this P-wave spin-singlet charmonium state.

**PACS number(s):** 13.85.Ni, 14.40.Lb, 12.39.Hg, 12.38.Bx.

Since the first charmonium, the  $J/\psi$ , was discovered thirty years ago, much effort has been made to explore it and its higher excited states with both theory and experiment. These studies have provided deep insights into the heavy quark-antiquark strong interaction, or, in other words, the application of quantum chromodynamics(QCD). Although much progress has been made, there are still many unsolved problems left in the study of quarkonium physics. For instance, in the charmonium sector, the  $c\bar{c}$  mass spectrum of the naive quark model prediction has not been completely confirmed experimentally yet. Below the open charm threshold, all expected charmonia have been identified in recent years, but experimental measurements of the physical natures of  $\eta'_c$  and  $h_c(^1P_1)$  are quite limited. The spin singlet states of heavy quarkonia pose an experimental challenge because they are not populated at lepton colliders. In hadron-hadron collision, the  $^1P_1$  state can be formed directly in many ways. The goal of this work is to analyze the possibility of detecting  $h_c(^1P_1)$  at the LHC.

$h_c$  is the ground state of the P-wave spin-singlet in the charmonium family. According to the QCD-based potential model prediction, to leading order of the spin-spin interaction the hyperfine splitting  $\Delta M_{hf}(M(^1P_1) - M(^3P_J))$  should be zero. Here, the spin-weighted average mass of P-wave triplet states  $M(^3P_J) = (M_{\chi_0}(^3P_0) + 3M_{\chi_0}(^3P_1) + 5M_{\chi_0}(^3P_2))/9 = 3525.30 \pm 0.04 \text{ MeV}$  and higher order corrections to the hyperfine splitting should be less than 1 MeV [1, 2, 3]. In 1995, the  $h_c$  signature, at about 3526 MeV, was first observed in the channel of  $h_c \rightarrow J/\psi\pi^0$  by the E760 Collaboration at the Fermilab [4]. Although this result was not confirmed by E835, which succeeded E760 with significantly higher statistics, the E835 Collaboration reported that they observed evidence of  $h_c$  via the  $h_c \rightarrow \eta_c\gamma$  process and obtained a resonance mass of  $3525.8 \pm 0.2 \pm 0.2 \text{ MeV}$  [5]. In the electron-positron collision, the CLEO Collaboration reported that they measured the mass of  $h_c$  at  $3525.28 \pm 0.19 \pm 0.12 \text{ MeV}$  via the decay of  $\psi(2S) \rightarrow \pi^0 h_c$  followed by  $h_c \rightarrow \eta_c\gamma$  at CESR [6, 7, 8], while the Belle Collaboration did not observe significant signal in the decay of  $B^\pm \rightarrow h_c K^\pm$  [9]. For a more detailed theoretical description of  $h_c$  and experimental progress in this respect, readers are referred to reviews [10, 11, 12].

To obtain more knowledge of the nature of  $h_c$ , a key point for experimentalists is to obtain enough  $h_c$  event data. The Large Hadron Collider (LHC) will be operational this year, which may supply a good opportunity to study quarkonium physics, including  $h_c$ .

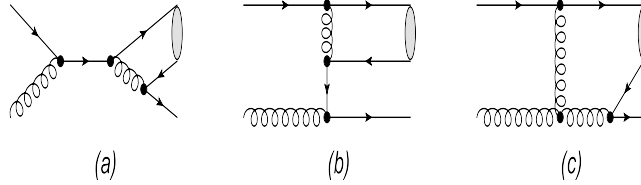


FIG. 1: Typical Feynman diagrams of  $h_c$  production in the extrinsic charm-induced process  $g + c \rightarrow h_c(^1P_1^{[1]}) + c$  in the color-singlet scheme.

With a luminosity of about  $10^{32} \sim 10^{34} \text{cm}^{-2} \text{s}^{-1}$  and a center of mass energy of  $10 \sim 14$  TeV, the LHC will produce copious charmonium data, which in principle will enable people to measure the  $h_c$  state more precisely. In the following we evaluate the  $h_c$  production rate at the LHC .

It is well-known that historically the so-called color-singlet model(CSM) [13, 14, 15, 16, 17] played a major role in the study of quarkonium physics and had great success in many respects. However, it failed to explain the Fermilab Tevatron data of charmonium large transverse momentum production. Hence, the color-octet mechanism (COM) was proposed and employed [18, 19], which is based on a solid framework, the nonrelativity QCD(NRQCD) [20]. The effective theory of NRQCD is widely accepted nowadays, although the validity of applying it to the charmonium phenomenological study is in some sense still vague. In the following calculation, nevertheless, both color-singlet and -octet contributions will be taken into account.

The differential cross section for  $h_c$  hadroproduction is formulated in a standard way,

$$\frac{d\sigma}{dp_T}(pp \rightarrow h_c + X) = \sum_{a,b} \int dx_a dy f_{a/p}(x_a) f_{b/p}(x_b) \frac{4p_T x_a x_b}{2x_a - \bar{x}_T e^y} \frac{d\hat{\sigma}}{dt}(a + b \rightarrow h_c + X), \quad (1)$$

where  $f_{a/p}$  and  $f_{b/p}$  denote the parton densities;  $s$ ,  $t$ , and  $u$  are Mandelstam variables at the parton level;  $y$  stands for the rapidity of produced  $h_c$ ;  $\bar{x}_T \equiv \frac{2m_T}{\sqrt{S}}$  with  $m_T = \sqrt{M^2 + p_T^2}$ ; and the capital  $\sqrt{S}$  and  $M$  denote the total energy of incident beam and the mass of  $h_c$ , respectively.

To leading order and with moderate transverse momentum, the dominant partonic subprocesses for  $h_c$  hadroproduction evidently include

$$g + g \rightarrow h_c(^1S_0^{[8]}) + g, \quad (2)$$

$$g + q(\bar{q}) \rightarrow h_c(^1S_0^{[8]}) + q(\bar{q}), \quad (3)$$

$$q + \bar{q} \rightarrow h_c(^1S_0^{[8]}) + g, \quad (4)$$

$$g + g \rightarrow h_c(^1P_1^{[1]}) + g, \quad (5)$$

$$g + c(\bar{c}) \rightarrow h_c(^1P_1^{[1]}) + c(\bar{c}), \quad (6)$$

where the first three represent the  $h_c$  production processes in the color-octet scheme, while the last two are through CSM. The process (6) is an ‘‘extrinsic charm’’ one, and its importance in charmonium hadroproduction was exhibited in Refs.[21, 22, 23]. To the lowest order of the strong coupling constant, expressions for the partonic differential cross section  $d\hat{\sigma}/dt$  of processes (2) to (5) were obtained in several previous studies [24, 25, 26, 27, 28], whereas the analytic expression for process  $g + c \rightarrow h_c(^1P_1^{[1]}) + c$ , as schematically shown in Figure 1, is still absent in the literature. It is worth mentioning that the ‘‘extrinsic charm’’ induced process  $c + \bar{c} \rightarrow h_c + g$  is omitted in our calculation since its numerical contribution is negligibly small.

For process (6), we commence with the calculation of the partonic process  $g + c \rightarrow (c\bar{c}) + c$ , then project the  $c\bar{c}$  matrix element onto the color-singlet  $^1P_1^{[1]}$  state. In calculating processes involving P-wave heavy quarkonium to leading order accuracy in relativistic expansion, one must expand the amplitude to the second order in powers of the relative momentum between the constituents of heavy quarkonium since the first order term gives no contribution. After taking the non-relativistic limit, it is then legitimate to take  $p_c = p_{\bar{c}} = P/2$ , one half of the charmonium momentum produced. For the outgoing  $h_c$ , one can employ the following projection operator:

$$v(p_{\bar{c}})\bar{u}(p_c) \longrightarrow \frac{-1}{2\sqrt{2}m_c} \left( \frac{P}{2} - \not{q} - m_c \right) \gamma_5 \left( \frac{P}{2} - \not{q} + m_c \right) \otimes \left( \frac{\mathbf{1}_c}{\sqrt{N_c}} \right), \quad (7)$$

where  $q$  is the relative momentum between two charm quarks,  $N_c = 3$ , and  $\mathbf{1}_c$  represents the unit color matrix. By writing the projector in a matter similar to (7), it is understood that  $M = 2m_c$  has been implicitly assumed.

After following the procedures mentioned above, it is straightforward to calculate the process (6), and the analytic result reads

$$\begin{aligned} \frac{d\hat{\sigma}}{dt} = & \frac{16\alpha_s^3\pi|R'(0)|^2}{27m_c(s-m_c^2)^2} \left( \frac{9t}{(s-m_c^2)^2m_c^2} + \frac{96(3m_c^2-5s)m_c^4}{(s-m_c^2)(t-m_c^2)^4} + \frac{32(39m_c^4-16sm_c^2-6s^2)m_c^2}{(s-m_c^2)^2(t-m_c^2)^3} \right. \\ & \left. - \frac{6(57m_c^4+14sm_c^2-7s^2)m_c^2}{(s+t-2m_c^2)(s-m_c^2)^4} + \frac{880m_c^8-631sm_c^6+119s^2m_c^4-201s^3m_c^2+25s^4}{(s-m_c^2)^4(t-m_c^2)m_c^2} \right) \end{aligned}$$

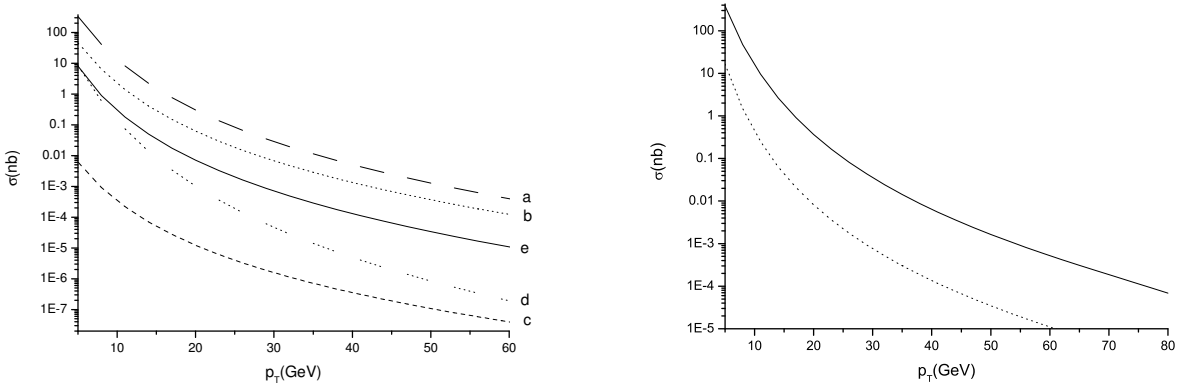


FIG. 2: The  $h_c$  production rates as a function of the transverse momentum lower bound  $p_T$  in  $pp$  collision at the center-of-mass energy  $\sqrt{S} = 14$  TeV. The left diagram demonstrates the integrated cross-sections of  $h_c$  production via processes (2) to (6) shown as lines a to e, respectively. The solid line in the right diagram represents the yield from the color-octet scheme, and the dashed line represents the yield from the color-singlet scheme.

$$\begin{aligned}
& + \frac{1177m_c^8 - 856sm_c^6 - 82s^2m_c^4 - 88s^3m_c^2 + 9s^4}{(s - m_c^2)^3(t - m_c^2)^2m_c^2} + \frac{2}{(s + t - 2m_c^2)^2} - \frac{256m_c^6}{(t - m_c^2)^5} \\
& + \frac{118m_c^8 - 379sm_c^6 + 141s^2m_c^4 - 161s^3m_c^2 + 25s^4}{(s - m_c^2)^5m_c^2} - \frac{8m_c^2}{(s + t - 2m_c^2)^3} \Big). \quad (8)
\end{aligned}$$

Here, the nonperturbative parameter,  $R'_{h_c}(0)$ , is the derivative of the Schrödinger radial wave function at the origin for  $h_c$ , which can be either inferred from phenomenological potential models or extracted from experimental data.

In our numerical evaluation, the input parameters are taken as follows:  $\sqrt{S} = 14$  TeV,  $m_c = M/2 = 1.78$  GeV, the value of the color-singlet matrix element  $\langle 0 | \mathcal{O}_1^{h_c}(^1P_1) | 0 \rangle = 0.32$  GeV<sup>5</sup> [29], the value of the color-octet matrix element  $\langle 0 | \mathcal{O}_8^{h_c}(^1S_0) | 0 \rangle = 9.8 \times 10^{-3}$  GeV<sup>3</sup> [28], and the pseudorapidity cut  $|\eta(h_c)| < 2.2$  is enforced according to the LHC experimental environment. In the calculation, the typical energy scale is set to be at  $m_T = \sqrt{M^2 + p_T^2}$ ; the strong coupling constant  $\alpha_s$  is running with transverse momentum. Both renormalization and factorization scales are evolved to the same point  $m_T$ , and the CTEQ5L [30] parton distribution function is employed. In Eq.(2), the relation between the NRQCD matrix element and the derivative of the Schrödinger radial wave function at the origin for the  $^1P_1$

TABLE I:  $h_c$  production rates with various transverse momentum lower bounds at the center-of-mass energy  $\sqrt{S} = 14\text{TeV}$  and an integrated luminosity of  $10 \text{ fb}^{-1}$  are presented. Taking into account the three main decay chains of  $h_c$ , i.e. 1)  $h_c \rightarrow \pi_0 J/\psi \rightarrow \mu^+ \mu^- \gamma \gamma$ , 2)  $h_c \rightarrow \eta_c \gamma \rightarrow p \bar{p} \gamma$  and 3)  $h_c \rightarrow \eta_c \gamma \rightarrow \gamma \gamma \gamma$ , the final experimentally detectable event numbers are given.

	color-singlet event				color-singlet event without charm sea effect				color-octet event			
$p_{Tcut}$	5 GeV	10 GeV	20 GeV	30 GeV	5 GeV	10 GeV	20 GeV	30 GeV	5 GeV	10 GeV	20 GeV	30 GeV
total	$1.65 \times 10^8$	$4.32 \times 10^6$	$8.14 \times 10^4$	$7.57 \times 10^3$	$8.41 \times 10^7$	$1.41 \times 10^6$	$1.02 \times 10^4$	$4.70 \times 10^2$	$3.78 \times 10^9$	$1.56 \times 10^8$	$3.67 \times 10^6$	$3.54 \times 10^5$
<i>Chain</i> <sub>1</sub>	$4.94 \times 10^4$	$1.30 \times 10^3$	$2.44 \times 10$	2.27	$2.52 \times 10^4$	$4.22 \times 10^2$	3.06	0.14	$1.13 \times 10^6$	$4.68 \times 10^4$	$1.10 \times 10^3$	$1.06 \times 10^2$
<i>Chain</i> <sub>2</sub>	$1.07 \times 10^5$	$2.81 \times 10^3$	$5.29 \times 10$	4.92	$5.47 \times 10^4$	$9.14 \times 10^2$	6.64	0.31	$2.45 \times 10^6$	$1.01 \times 10^5$	$2.38 \times 10^3$	$2.30 \times 10^2$
<i>Chain</i> <sub>3</sub>	$1.97 \times 10^4$	$5.19 \times 10^2$	9.76	0.91	$1.01 \times 10^4$	$1.69 \times 10^2$	1.23	0.06	$4.53 \times 10^5$	$1.87 \times 10^4$	$4.40 \times 10^2$	$4.24 \times 10$

state, i.e.,

$$|R'(0)| = \sqrt{\frac{2\pi}{27} \langle 0 | \mathcal{O}_1^{h_c} ({}^1P_1) | 0 \rangle}, \quad (9)$$

is adopted. Note that among the inputs, the charm quark mass  $m_c$  is taken to be one half of the  $h_c$  mass for simplicity, i.e., the constituent quark mass, which we find may increase the final result by some 30% from that found when taking  $m_c$  to be 1.5 GeV.

The numerical results of the integrated cross section for different  $p_T$  lower bounds are given in Figure 2. From the figure, it can be found that the contribution from COM is about two orders of magnitude larger than that from CSM in almost every transverse momentum region. Among the three color-octet processes, the contribution from process (2) dominates over the other two. Of the two color-singlet processes, the yield from process (6) overshoots that from process (5) in the large transverse momentum region, in spite of the suppression of the extrinsic charm distribution. Because of the big gap between the yields from the color-singlet and color-octet, one result of this calculation is that the experimental measurement may tell whether the color-octet estimate of  $h_c$  production is reliable or not.

In experiment the  $h_c$  can be reconstructed from its three dominant decay modes, which are

$$h_c \rightarrow \pi_0 J/\psi \rightarrow \mu^+ \mu^- \gamma \gamma, \quad (10)$$

$$h_c \rightarrow \eta_c \gamma \rightarrow p \bar{p} \gamma, \quad (11)$$

$$h_c \rightarrow \eta_c \gamma \rightarrow \gamma \gamma \gamma. \quad (12)$$

Of these decay chains,  $J/\psi$  decays into  $\mu^+ \mu^-$  with a branching ratio of 6% [31],  $\pi^0$  almost

completely decays into  $\gamma\gamma$ , and  $\eta_c$  decays into  $p\bar{p}$  with a branching fraction of 0.13% and into  $\gamma\gamma$  with a ratio of 0.024% [31]. The branch fractions of  $h_c \rightarrow J/\psi\pi^0$  and  $h_c \rightarrow \eta_c\gamma$  are theoretically estimated to be about 0.5% [32] and 50% [33, 34, 35, 36], respectively. For the  $h_c \rightarrow J/\psi\pi^0$  process, although the  $\pi^0$ s produced are energetic, their decays to two photons can be well resolved when the  $\pi^0$  momentum is less than 40 GeV [37]. Considering the decay rates of  $h_c$  to these experimentally measurable modes, in Table I we present the event numbers of the decay chains (10)-(12) with different transverse momentum lower bounds and in the LHC experiment environment, that is, a 14 TeV colliding energy, a  $10 \text{ fb}^{-1}$  integrated luminosity and a pseudo-rapidity cut  $|\eta(h_c)| < 2.2$ . From the table we see that even the  $h_c$  produced with a lower transverse momentum bound of 10 GeV, in which region the experimental detection efficiency becomes high, there will be millions of events coming out in its three dominant decay modes, from both the color-singlet and -octet schemes. In the table, we also present the color-singlet contribution without the charm sea effects. One may find that the charm sea-induced process contributes at least half of the total color-singlet yield with various transverse momentum lower bounds.

In conclusion, we have evaluated the  $h_c$  direct production rate at the LHC, where the  $h_c$  indirect yields are much less than the direct ones according to a similar analysis for  $h_c$  production at HERA-b [27]. Our calculation is performed to leading order of the strong coupling constant  $\alpha_s$  and to second order in the relative velocity  $v^2$  expansion. Both color-singlet and -octet production schemes are taken into account in this work. We find that there will be enough  $h_c$  yields at the LHC for a precise measurement on the nature of this P-wave spin singlet. Although as usual the high order corrections may induce some uncertainties in the calculation, as an order-of-magnitude estimate our results should hold. Due to the large discrepancy between predictions from the color-singlet and color-octet schemes, the experimental measurement of the  $h_c$  production rate at the LHC may tell to what degree the color-octet mechanism plays a role in charmonium production as well.

Finally, as we were studying this issue, there appeared a similar work on the web [38]. The main difference between this work and Ref.[38] is the inclusion of the extrinsic charm contribution process (6). Since the necessary definitions in several places of Ref. [38] are not clear, it is hard to make a direct comparison of our results with those given in the reference.

## Acknowledgments

This work was supported in part by the National Natural Science Foundation of China(NSFC) under the grants 10821063 and 10775179, by CAS Key Project on " $\tau$ -Charm Physics(NO.KJCX2-yw-N29) and by the Scientific Research Fund of GUCAS (NO.O85102BN00).

---

- [1] T. Appelquist, R.M. Barnett and K.D. Lane, *Ann. Rev. Nucl. Part. Sci.* **28**, 387(1978).
- [2] S. Godfrey and J.L. Rosner, *Phys. Rev.* **D66**, 014012(2002).
- [3] D. N. Joffe, Ph.D thesis, Northwestern University, 2004; hep-ex/0505007.
- [4] E760 Collaboration, T.A. Armstrong, *et al.*, *Phys. Rev.* **D52**, 4839(1995).
- [5] E835 Collaboration, M. Andreotti, *et al.*, *Phys. Rev.* **D72**, 032001(2005).
- [6] CLEO Collaboration, J.L. Rosner, *et al.*, *Phys. Rev. Lett.* **95**, 102003(2005).
- [7] CLEO Collaboration, P. Rubin, *et al.*, *Phys. Rev.* **D72**, 092004(2005).
- [8] CLEO Collaboration, S. Dobbs, *et al.*, *Phys. Rev. Lett.* **101**, 182003(2008).
- [9] Belle Collaboration, F. Fang, *et al.*, *Phys. Rev.* **D74**, 012007(2006).
- [10] T. Barnes, T.E. Browder, and S.F. Tuan, e-Print: hep-ph/0408081.
- [11] Quarkonium Working Group, N. Brambilla, *et al.*, CERN Yellow Report, e-Print: hep-ph/0412158.
- [12] D.M. Asner, *et al.*, IHEP-PHYSICS-REPORT-BES-III-2008-001, arXiv:0809.1869.
- [13] T.A. DeGrand and D. Toussiant, *Phys. Lett.* **B89**, 256(1980).
- [14] M. Wise, *Phys. Lett.* **B89**, 229(1980).
- [15] J.H. Kuhn, S. Nussinov, and R.Z. Ruckle, *Z. Phys.* **C5**, 117(1980).
- [16] C.H. Chang, *Nucl. Phys.* **B172**, 425(1980).
- [17] E.L. Berger and D.L. Jones, *Phys. Lett.* **B121**, 61(1983); *ibid*, *Phys. Rev.* **D23**, 1521(1981).
- [18] G.T. Bodwin, E. Braaten, T.-C. Yuan, and G.P. Lepage, *Phys. Rev.* **D46**, R3703(1992).
- [19] E. Braaten and S. Fleming, *Phys. Rev. Lett.* **74**, 3327(1995).
- [20] G.T. Bodwin, E. Braaten, and G.P. Lepage, *Phys. Rev. D* **51**, 1125 (1995).
- [21] K. Hagiwara, W. Qi, C.F. Qiao and J.X. Wang, the proceedings of 34th International Conference on High Energy Physics, Philadelphia, 2008; [arXiv:0705.0803].



- [22] C.-F. Qiao, J. Phys. **G29**, 1075(2003); [hep-ph/0202227].
- [23] A.P. Martynenko and V.A. Saleev, Phys. Lett. **B343**, 381(1995).
- [24] M.M. Meijer, J. Smith and W.L. van Neerven Phys. Rev. **D77**, 034014 (2008).
- [25] R. Gastmans, W. Troost and T. Wu, Nucl. Phys. **B291**, 731 (1987).
- [26] M. Klasen, B. Kniehl, L. Mihaila, and M. Steinhauser, Phys. Rev. **D68**, 034017 (2003).
- [27] C.-F. Qiao and C.Z. Yuan, Phys. Rev. **D63**, 014007(2001).
- [28] P.L. Cho and A.K. Leibovich, Phys. Rev. D **53**, 150(1996); Phys. Rev. **D53**, 53(1996).
- [29] M. Mangano and A. Petrelli, Phys. Lett. **B352**, 445(1995).
- [30] CTEQ Collaboration, H.L. Lai *et al.*, Eur. Phys. J. **C12**, 375(2000).
- [31] Particle Data Group(PDG), C. Amsler, *et al.*, Phys. Lett. **B667**, 1(2008).
- [32] Y.P. Kuang S.F. Tuan and T.M. Yuan Phys. Rev. **D37**, 1210(1988).
- [33] S. Godfrey and J.L. Rosner, Phys. Rev. **D66**, 014012(2002), and references therein.
- [34] Y.P. Kuang, S.F. Tuan and T.M. Yan, Phys. Rev. **D37**, 1210(1988).
- [35] P. Ko, Phys. rev. **D52**, 1710(1995).
- [36] M. Suzuki, Phys. Rev. **D66**, 037503(2002).
- [37] Private communication with G.M.Chen (CMS Collaboration).
- [38] K. Sridhar, Phys. Lett. **B674**, 36(2009); [arXiv:0812.0474].